

Carbon Monoxide Restructuring of Palladium Crystallite Surfaces

ROBERT F. HICKS,¹ HAIHUA QI,² ANDREW B. KOOH, AND LAWRENCE B. FISCHER

UCLA Chemical Engineering Department, 5531 Boelter Hall, Los Angeles, California 90024-1592

Received January 5, 1990; revised February 22, 1990

Six palladium on alumina catalysts were prepared with dispersions between 3 and 86%. Over several cycles of carbon monoxide exposure at 25°C and reduction at 300°C, the carbon monoxide, oxygen, and hydrogen adsorption capacities decreased by 20 to 50%. The loss of surface sites was higher on the small crystallites. The adsorption capacity recovered with oxidation at 550°C and reduction at 300°C. The carbon monoxide and oxygen treatments did not affect the hydrogen solubility in the palladium particles. However, infrared spectroscopy of adsorbed carbon monoxide revealed that the surface structure changed with the gas treatments. When the catalyst was converted from the carbon monoxide-exposed state to the oxidized state, the band at 1970 cm⁻¹ for bridge-bonded carbon monoxide on (100) facets decreased, while the band at 2095 cm⁻¹ for linearly bonded carbon monoxide on low-coordination sites increased. In some instances, the bands at 1995 and 1885 cm⁻¹ increased after oxidation. These latter features are tentatively assigned to bridged and threefold-bridged bonded carbon monoxide adjacent to linearly bonded carbon monoxide on low coordination sites. A model is presented to explain these results: cycles of carbon monoxide exposure and reduction smooth the crystallite surfaces into well-ordered facets, whereas cycles of oxidation and reduction roughen the surfaces. © 1990 Academic Press, Inc.

INTRODUCTION

Carbon monoxide adsorption is a valuable probe for characterizing the structure of metallic catalysts. The dispersion is calculated from the amount adsorbed at saturation (1–4). The morphology of the crystallite surfaces is assessed by infrared spectroscopy of adsorbed carbon monoxide (4–8). Peaks observed in the infrared spectrum correspond to carbon monoxide bonding at sites with specific arrangements of metal atoms. The configuration of the site is deduced by comparison to infrared spectra of carbon monoxide adsorbed on single crystals (9–11). The distribution of peaks in the spectrum is indicative of the distribution of sites on the crystallites. Assuming that the metal particles are unchanged by exposure to carbon monoxide, these experiments, when

combined with measurements of catalytic reaction rates, provide a means of evaluating the relationship between the structure and the reactivity of supported metals.

In a study of supported palladium catalysts, Chou and Vannice (12) found that the adsorption capacity of the metal decreases over several cycles of carbon monoxide adsorption at 25°C and reduction at 400°C. The adsorption capacity did not recover following oxidation at 300 to 500°C and reduction at 300°C. These treatments should have removed the adsorbed carbon monoxide and any carbon formed by carbon monoxide disproportionation (13–16). The results of Chou and Vannice suggest that carbon monoxide adsorption alters the structure of the palladium crystallites.

We have further investigated the effect of exposing palladium on alumina to carbon monoxide at room temperature. Catalysts of different metal loading and dispersion were alternately treated with carbon monoxide at 25°C and with oxygen at 300 to 600°C. After

¹ To whom correspondence should be addressed.

² Current address: Department of Chemistry, Nanjing University, Nanjing, China.

TABLE 1

Properties of the Palladium on Alumina Catalysts

| Sample number | Oxidation temperature (°C) | Palladium loading (%) | Ratio of CO adsorbed to total palladium ^a (%) |
|---------------|----------------------------|-----------------------|--|
| 11b | 700 | 0.20 | 86 |
| 11c | 900 | 0.20 | 59 |
| 12b | 700 | 0.46 | 59 |
| 12c | 900 | 0.46 | 19 |
| 13b | 700 | 2.30 | 11 |
| 13c | 900 | 2.30 | 3 |

^a Uptake of CO after initial oxidation and reduction.

each treatment, the catalysts were reduced at 300°C and characterized by carbon monoxide, oxygen, and hydrogen adsorption, by hydrogen absorption, by infrared spectroscopy of adsorbed carbon monoxide, and by temperature-programmed oxidation. We have found that the adsorption capacity and the infrared spectrum of adsorbed carbon monoxide change dramatically as the catalyst is cycled between carbon monoxide exposure and oxidation.

EXPERIMENTAL

Materials

The catalysts were prepared by room temperature ion exchange of H_2PdCl_4 with Degussa aluminum oxide "C" (17). The alumina was first calcined in air at 1000°C for 24 h (surface area 83 m²/g). After ion exchange, the samples were filtered from solution, washed with distilled water, dried at 105°C overnight, and oxidized at 700 or 900°C for 2 h. Then the samples were stored in a desiccator. The weight percents of palladium in the oxidized samples were determined by inductively coupled plasma emission spectroscopy. The sample number, the oxidation temperature, the palladium loading, and the initial amount of adsorbed carbon monoxide are shown for each catalyst in Table 1.

The gases used were Matheson research purity carbon monoxide (99.99%) and Liquid Air Corp. hydrogen (99.995%), helium

(99.995%), and oxygen (99.995%). The carbon monoxide impurities were less than 5 ppm CO₂ and 26 ppm total carbon in hydrocarbons. The carbon monoxide was added to the glass chemisorption apparatus by passing it through glass beads held at 300°C and then through a 13X molecular sieve trap immersed in dry ice (−78°C). For the gas treatments using the pulse-flow apparatus, the gases were passed through 13X molecular sieve traps immersed in dry ice. The carbon monoxide, hydrogen, and helium were also passed through an oxygen adsorbent (Alltech) located before the cold traps.

Methods

The uptake of carbon monoxide and oxygen on each sample was determined by volumetric chemisorption (1). From 1 to 3 g of catalyst was pelletized, crushed, and sieved to 32–60 mesh size. The pellets were placed in a quartz chamber, reduced in 200 cm³/min hydrogen at 300°C for 1 h, and then cooled from 300 to 25°C in 1×10^{-6} Torr vacuum (1 Torr = 133 N/m²). The carbon monoxide adsorption isotherm was measured at 25°C in the pressure range from 10 to 150 Torr. The linear dependence of the gas uptake on pressure at the higher pressures was back-extrapolated to zero to give the amount adsorbed.

After recording the first isotherm, the sample was briefly exposed to air and reduced in 200 cm³/min hydrogen at 300°C for 1 h. Then the carbon monoxide uptake was measured. This procedure was repeated many times until the amount adsorbed remained constant. The condition of the catalyst at this stage is denoted as the "CO cycled" state. Next, the sample was oxidized in 200 cm³/min oxygen at 550°C for 1 h and reduced in 200 cm³/min hydrogen at 300°C for 1 h. Then the carbon monoxide adsorption isotherm was recorded again. This procedure was also repeated until the amount adsorbed remained constant. The condition of the catalyst at this stage is denoted as the "oxidized" state. After completing each of the cycles of carbon monoxide exposure and

oxidation, the sample was reduced at 300°C and the oxygen adsorption isotherm was recorded.

The hydrogen solubility was determined on each sample to assess the effect of carbon monoxide exposure on the bulk properties of the palladium particles. These measurements were performed in the volumetric chemisorption apparatus, using the back-sorption technique described by Boudart and Hwang (18). The hydrogen solubility was measured after three cycles of carbon monoxide adsorption at 25°C and reduction at 300°C (CO cycled), and again after two cycles of oxidation at 600°C and reduction at 300°C (oxidized). After the last reduction step, the sample was cooled in flowing hydrogen to 25°C and held for 10 min. The chamber was pumped out to 1×10^{-5} Torr over 10 min. Then a known amount of hydrogen was admitted to the chamber such that 200 Torr remained in the gas after several hours of contact with the catalyst. The amount of hydrogen adsorbed at 25°C and 200 Torr was calculated from a material balance on the system.

Infrared spectra of adsorbed carbon monoxide of the CO cycled and the oxidized catalyst samples were recorded. A 0.1-g sample was pressed into a 13-mm-diameter wafer and placed in a glass cell. The wafer was treated as described in the chemisorption experiments. At room temperature, small aliquots of carbon monoxide, 0.5 to 2.5×10^{-7} mol, were dosed into the chamber and the infrared spectrum was recorded. The intensity of the infrared bands increased linearly with each dose until the saturation point was reached (4). The spectra shown are for saturation only. The infrared spectra were recorded on a Digilab FTS-40 spectrometer with a DTGS detector at 4-cm^{-1} resolution and coadding 64 scans.

Adsorption experiments were performed in a pulse-flow apparatus equipped with on-line gas chromatography. The concentrations of oxygen, carbon monoxide, and carbon dioxide exiting the reactor were measured with a Carbosphere column (Alltech)

and a thermal conductivity detector. Each catalyst sample used in these experiments had been subjected to many cycles of carbon monoxide adsorption, reduction and oxidation in the chemisorption apparatus. First, the sample was converted to the oxidized state: it was heated in 50 cm³/min oxygen from 25 to 600°C in 20 min, held at 600°C for about 30 min until no more carbon dioxide evolved, cooled to 300°C, purged with helium, and reduced at 300°C for 20 min. These oxidation and reduction steps were repeated to ensure that the amount of surface carbon was reduced to a minimum. The sample was then cooled to 50°C and reheated in 50 cm³/min oxygen from 50 to 600°C at 11°C/min. The temperature-programmed oxidation of surface carbon to carbon dioxide was recorded during the heating cycle. Next, the sample was reduced at 300°C, cooled in hydrogen to 50°C, purged with 30 cm³/min helium, and pulsed with oxygen and hydrogen. The dispersion was calculated from the number of oxygen and hydrogen pulses adsorbed at 50°C, assuming $\frac{3}{4}$ O₂ and $\frac{3}{2}$ H₂ are consumed per surface palladium atom (Pd_s) (3, 4). The value measured at this stage of the experiment corresponds to the dispersion of the catalyst in the oxidized state.

The catalyst was converted to the CO-cycled state in the pulse-flow apparatus as follows: it was exposed to 10 cm³/min carbon monoxide at 25°C for 30 min, heated in 50 cm³/min hydrogen from 25 to 300°C at 6°C/min, reduced at 300°C for 20 min, and cooled in hydrogen to 50°C. At 50°C, the palladium dispersion was determined by pulsing the sample with oxygen and hydrogen. This sequence of treatments was repeated three times. The hydrogen-oxygen titration after the third cycle gave the dispersion of the catalyst in the CO cycled state. After this last titration, the sample was heated in 50 cm³/min oxygen from 50 to 600°C at 11°C/min and held at 600°C for 20 min. The temperature-programmed oxidation of surface carbon to carbon dioxide was recorded during the heating cycle. Then the sample was cooled to 300°C, helium purged

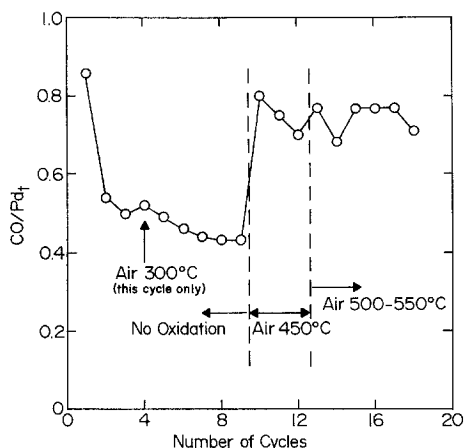


FIG. 1. The dependence of the ratio of carbon monoxide adsorbed to total palladium on the number of cycles of carbon monoxide adsorption at 25°C, oxidation at 300 to 600°C (cycles 4, 10–18) and reduction at 300°C for sample 11b.

for 10 min, reduced in 50 cm³/min hydrogen at 300°C for 20 min, and cooled in hydrogen to 50°C. At 50°C, the catalyst was titrated with oxygen and hydrogen. This cycle of temperature-programmed oxidation, reduction, and H₂–O₂ titration was repeated twice.

RESULTS AND DISCUSSION

Effect of Gas Treatments on the Adsorption Capacity

Figure 1 shows the change in the carbon monoxide uptake of sample 11b with cycling between carbon monoxide adsorption, reduction, and oxidation in the chemisorption apparatus. During the first three cycles, the sample is alternately exposed to carbon monoxide and reduced at 300°C. The number of carbon monoxide molecules adsorbed per total palladium atoms (CO/Pd_t) falls from 0.86 to 0.48. This is similar to the drop in adsorption capacity observed by Chou and Vannice (12) during their adsorption experiments. In the fourth cycle, sample 11b is oxidized at 300°C and reduced at 300°C prior to adsorption. Only a small amount of the carbon monoxide uptake is recovered by this treatment. During five more cycles

of reduction and adsorption, the amount adsorbed slowly declines to 0.40. In the 10th through the 18th cycles, the catalyst is oxidized at 450 to 550°C, and the adsorption capacity increases to 0.76 CO/Pd_t. Oxidation at 550°C is required to stabilize the carbon monoxide uptake against repeated cycling.

The oxygen uptake is affected in the same fashion by the gas treatments. After the last cycle of carbon monoxide adsorption and reduction (cycle 9, Fig. 1), sample 11b adsorbs 0.32 O/Pd_t, whereas after the last cycle of carbon monoxide adsorption, oxidation at 550°C and reduction at 300°C (cycle 18, Fig. 1), sample 11b adsorbs 0.74 O/Pd_t. These values are in good agreement with the carbon monoxide uptakes, assuming one carbon monoxide molecule and one O atom are adsorbed per Pd_s.

The pulse-flow apparatus was used to explore the effects of different exposures to carbon monoxide and oxygen on the adsorption capacity of sample 13b. The results are summarized in Table 2. In the first cycle, after oxidation at 500°C and reduction at 300°C, the sample adsorbs 0.105 CO/Pd_t. Three additional cycles of reduction at

TABLE 2

Changes in the Palladium Dispersion on Exposing Sample 13b to Different Gas Treatments

| Cycle | Treatment ^a | | | Ratio of CO adsorbed to total palladium (%) | Palladium dispersion ^b (%) |
|------------|------------------------|----------------|------------------|---|---------------------------------------|
| | Time (h) | Gas | Temperature (°C) | | |
| 1 | 1.3 | O ₂ | 500 | 10.5 | |
| 5 | 0.3 | O ₂ | 25 | 10.0 | |
| 6 | 1.0 | CO | 25 | 6.3 | |
| 7 | 1.5 | CO | 25 | 5.5 | |
| 8 | 1.0 | CO | 25 | 5.3 | |
| 9 | 1.0 | O ₂ | 500 | 6.4 | |
| 10 | 1.0 | O ₂ | 550 | 7.3 | 7.2 |
| New sample | | | | | |
| 11 | 1.2 | O ₂ | 600 | | 11.6 |
| 12 | 0.5 | CO | 25 | | 6.2 |
| 13 | 0.5 | CO | 25 | | 6.1 |
| 14 | 0.3 | O ₂ | 600 | | 8.1 |
| 15 | 0.3 | O ₂ | 600 | | 8.8 |

^a After each treatment the sample was reduced 1 h at 300°C.

^b Dispersion measured by H₂–O₂ titration at 50°C.

300°C and pulse adsorption of carbon monoxide at 25°C (cycles 2–4, not shown in the table) do not change the amount of carbon monoxide adsorbed. This proves that adsorbed carbon monoxide is not responsible for the drop in adsorption capacity.

During the volumetric chemisorption experiments, the samples were briefly exposed to air before each reduction step. To see if this lowers the adsorption capacity, sample 13b was exposed to oxygen at 25°C in the fifth cycle. No change in the carbon monoxide uptake is observed with this treatment. In the sixth through the eighth cycles, sample 13b was repeatedly contacted with flowing carbon monoxide at 25°C and reduced at 300°C. This time the amount of carbon monoxide adsorbed decreases from 0.100 to 0.053 CO/Pd_t. These experiments demonstrate that the adsorption capacity drops only if the catalyst is exposed to a continuous pressure of carbon monoxide at room temperature.

As shown in the 9th and 10th cycles, oxidation of sample 13b at 500 and 550°C increases the carbon monoxide uptake to 0.073 CO/Pd_t. This is 70% of the initial adsorption capacity. When these same experiments are conducted in the volumetric chemisorption apparatus, the adsorption capacity is fully recovered by oxidation. The main difference between the pulse-flow experiment and the chemisorption experiment is that the carbon monoxide pressure is 760 Torr in the former case, but between 10 and 150 Torr in the latter case. Evidently, exposing the catalyst to a higher pressure of carbon monoxide makes it more difficult to restore the palladium to the oxidized state.

In the 10th cycle, sample 13b was pulsed with carbon monoxide and titrated with hydrogen and oxygen. The dispersion measured by H₂–O₂ titration equals the ratio of carbon monoxide adsorbed to total palladium. This corresponds to an adsorption stoichiometry of 1 CO/Pd_s, in agreement with previous studies of supported palladium catalysts (3, 4). The bottom half of Table 2 reports the results of a second series

of tests in which the metal surface was titrated with hydrogen and oxygen after each cycle. As the sample is oxidized, exposed to carbon monoxide, and oxidized again, the dispersion changes from 11.6 to 6.1 to 8.8%. These dispersions are within 20% of the ratios of carbon monoxide adsorbed to total palladium measured after the same treatments in cycles 1 to 10. Since the amounts of carbon monoxide, oxygen, and hydrogen adsorbed are equally affected, the change in adsorption capacity with the carbon monoxide and oxygen treatments results from a change in the number of exposed palladium atoms.

The effects of CO cycling and oxidation on the adsorption capacities of the different palladium catalysts are shown in Table 3. Assuming that one oxygen atom is adsorbed per surface palladium atom, the oxygen uptakes measured by volumetric chemisorption and the dispersions measured by pulsed H₂–O₂ titration agree to within experimental error. However, the carbon monoxide uptakes measured by volumetric chemisorption and the dispersions measured by pulsed H₂–O₂ titration do not agree as well. The ratio of carbon monoxide molecules adsorbed per surface palladium atom ranges from 1.00 to 1.81. This discrepancy may be due to the adsorption of carbon monoxide in excess of monolayer coverage, either on the metal or on the support, during equilibration of the sample with the carbon monoxide gas in the chemisorption apparatus. When carbon monoxide is adsorbed onto the catalyst in the pulse-flow apparatus, the uptake equals the expected value of 1 CO/Pd_s (see cycle 10, Table 2).

As shown in Table 3, all the samples are affected by CO cycling. The percentage decrease in adsorption capacity is about the same for carbon monoxide and oxygen adsorption and for hydrogen and oxygen titration. This affirms our conclusion that CO cycling reduces the amount of exposed palladium. Oxidation at 550°C increases the adsorption capacity to within 15% of the value recorded before CO cycling. The data in the

TABLE 3

Changes in the Adsorption Capacity with CO Cycling and Oxidation of the Palladium on Alumina Catalysts

| Sample number | Ratio of CO adsorbed to total palladium (%) | | | Ratio of O adsorbed to total palladium (%) | | Palladium dispersion ^a | | Decrease in dispersion ^b (%) |
|---------------|---|-----------|----------|--|----------|-----------------------------------|----------|---|
| | Initial | CO cycled | Oxidized | CO cycled | Oxidized | CO cycled | Oxidized | |
| 11b | 86 | 40 | 76 | 32 | 74 | 28 | 70 | 60 |
| 11c | 59 | 37 | 69 | 25 | 48 | 26 | 47 | 45 |
| 12b | 59 | 29 | 51 | 16 | 44 | 16 | 37 | 57 |
| 12c | 19 | 10 | 15 | 6 | 13 | 8 | 15 | 47 |
| 13b | 11 | 8 | 12 | 6 | 9 | 6 | 9 | 33 |
| 13c | 3 | 2.5 | 3 | 2 | 3 | 2 | 3 | 33 |

^a Dispersion measured by H₂-O₂ titration at 50°C.^b Decrease = (oxidized - cycled)/oxidized.

last column of Table 3 reveal that the loss of adsorption sites is slightly dependent on particle size. The percentage decrease in dispersion is greater on the smaller particles.

One possible explanation for the drop in adsorption capacity with exposure to carbon monoxide is that carbon monoxide disproportionates, depositing carbon on the surface of the palladium particles (13-16). This reaction is unlikely at room temperature, but could occur when the adsorbed carbon monoxide is heated in hydrogen to 300°C. To check this possibility, the amount of carbon on the samples was analyzed by temperature-programmed oxidation. A series of temperature-programmed oxidation spectra for sample 12b is shown in Fig. 2. Spectrum (a) was recorded after oxidation at 600°C and reduction at 300°C. A burst of carbon dioxide appears at 350°C, after which a small amount continues to evolve during oxidation at 600°C. The amount of carbon dioxide produced corresponds to 0.09 adsorbed carbon atoms per total palladium atoms (C/Pd_i). Spectrum (b) was recorded after converting the sample into the CO cycled state. The carbon dioxide now appears at 390°C, 40°C higher than in spectrum (a). Nevertheless, the same amount of carbon dioxide is produced. Spectrum (c)

was recorded after spectrum (b) and reduction of the catalyst at 300°C. In this case, the peak maximum shifts down to 340°C, and the amount of carbon dioxide produced corresponds to 0.05 C/Pd_i. Since equal amounts of carbon are oxidized off the sample before and after carbon monoxide cycling, no carbon is deposited as a result of this treatment. Therefore, the loss of adsorption capacity upon exposure to carbon monoxide is not due to adsorbed carbon.

The amount of carbon dioxide desorbed from sample 12b during temperature-programmed oxidation averages 3.3×10^{-6} mol/g. This quantity may be compared to 1.3×10^{-6} mol/g carbon dioxide desorbed from the alumina support and between 1.0 and 3.0×10^{-6} mol/g carbon dioxide desorbed from the other catalyst samples during the same sequence of treatments. Since the amount desorbed varies over a narrow range from one sample to the next and is close to the value for the alumina, it is concluded that the carbon dioxide arises from the oxidation of carbon bound to the alumina support. The carbon dioxide peak in the temperature-programmed oxidation spectrum of the support occurs at 465°C. By contrast, sample 12b exhibits a peak maximum at 345 or 390°C. The lower temperature of the peak means that the palladium cata-

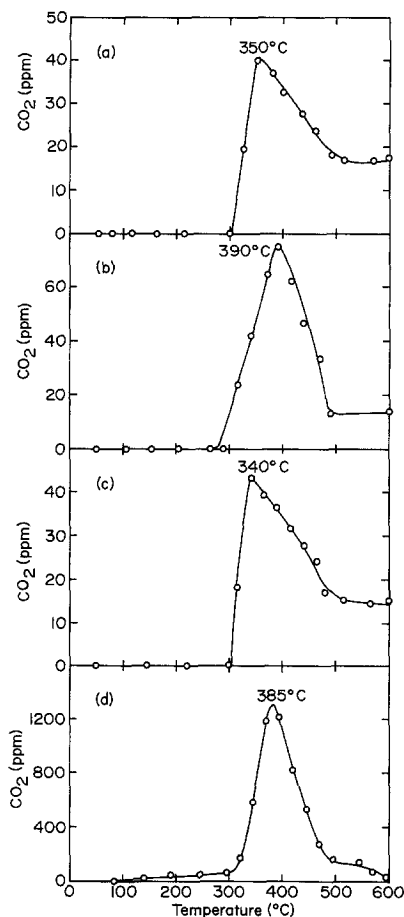


FIG. 2. Temperature-programmed oxidation spectra for sample 12b: (a) after oxidation at 600°C and reduction at 300°C; (b) after three cycles of carbon monoxide exposure at 25°C and reduction at 300°C; (c) after spectrum (b) and reduction at 300°C; and (d) after carbon monoxide exposure at 300°C and reduction at 300°C.

lyzes the oxidation of the carbon off the alumina.

The following experiment was conducted to document what occurs when carbon is deposited by carbon monoxide disproportionation. The sample was heated in 10 cm³/min carbon monoxide from 25 to 300°C at 6°C/min, held in 10 cm³/min carbon monoxide at 300°C for 1 h, helium purged at 300°C for 3 h to remove the adsorbed carbon monoxide, cooled to room temperature, and titrated with hydrogen and oxygen. A temperature-programmed oxidation spectrum, Fig.

2d, was then obtained. After this oxidation, the sample was reduced and titrated with hydrogen and oxygen. The amount of carbon deposited from carbon monoxide at 300°C far exceeds the amount of surface palladium lost. The temperature-programmed oxidation spectrum indicates a net accumulation of 0.85 C/Pd_t (after correcting for the support adsorption). This may be contrasted to the decrease in palladium dispersion from 24 to 7%. Furthermore, the loss of adsorption sites is irreversible, since oxidation at 600°C only increases the dispersion to 11%. The percentage change in adsorption capacity due to carbon monoxide exposure at 300°C is greater than that due to carbon monoxide exposure at 25°C. In the latter case, carbon monoxide exposure decreases the dispersion from 37 to 16%, and subsequent oxidation increases the dispersion to 24%.

Ichikawa *et al.* (14) investigated carbon monoxide disproportionation on silica-supported palladium. On two samples with dispersions of 79 and 88%, the adsorption capacity decreased over several cycles of carbon monoxide adsorption and desorption. On one sample with a dispersion of 38%, the adsorption capacity remained constant during the cycling. The loss of surface sites on the highly dispersed palladium was approximately equal to the amount of carbon deposited by carbon monoxide disproportionation. In contrast to their results, we find that catalysts with low and high dispersions exhibit lower adsorption capacity after exposure to carbon monoxide. Moreover, the amount of carbon deposited bears no relation to the change in the number of surface sites. The main difference between their study and ours is the way the palladium was exposed to carbon monoxide. Ichikawa *et al.* (14) cycled the catalysts between 25 and 400°C in an evacuated system with carbon monoxide present on the surface of the palladium particles. Under these conditions, exposed palladium atoms will be lost only by the decomposition of adsorbed carbon monoxide into adsorbed carbon.

TABLE 4
Effect of CO Cycling and Oxidation on the
Hydrogen Solubility

| Sample number | Palladium dispersion ^a (%) | Ratio of H absorbed to total palladium ^b (%) | |
|---------------|---------------------------------------|---|----------|
| | | CO cycled | Oxidized |
| 11b | 70 | 26 | 29 |
| 11c | 47 | 50 | 53 |
| 12b | 37 | 63 | 70 |
| 12c | 15 | 46 | 49 |
| 13b | 9 | — | — |
| 13c | 3 | 73 | 70 |

^a Oxidized state.

^b Amount of hydrogen absorbed at 25°C on palladium precovered with hydrogen.

The spectra in Fig. 2 reveal a correlation between the nature of the treatment and the temperature for the maximum rate of carbon dioxide production. After oxidation and reduction, sample 12b exhibits a maximum rate at 345°C (spectra (a) and (c)), whereas after CO cycling, or after exposure to carbon monoxide at 300°C and reduction at 300°C, sample 12b exhibits a maximum rate at 390°C (spectra (b) and (d)). These data show that the palladium in the CO-cycled state catalyzes the oxidation of adsorbed carbon at a slower rate than the palladium in the oxidized state.

Another possible explanation for the drop in adsorption capacity with exposure to carbon monoxide is that the palladium particles agglomerate. This hypothesis can be checked by measuring the hydrogen solubility in the particles (18). If the particle size increases on exposure to carbon monoxide, then the uptake of hydrogen in the bulk should go up. Table 4 shows the amounts of hydrogen back-absorbed into the catalyst samples after they had been covered with chemisorbed hydrogen. The number of hydrogen atoms absorbed varies from 26 to 73% of the total number of palladium atoms. Samples with smaller metal particles take up less because fewer metal atoms are below

the surface. On the large particles, the solubility equals the value observed for bulk crystals of palladium (19). As shown in Table 4, the hydrogen solubilities in the palladium in the CO-cycled and oxidized states are within 6% of one another. This difference is within the experimental error of the measurement. Therefore, the metal crystallites do not agglomerate in the presence of carbon monoxide gas at room temperature.

In summary, subjecting palladium particles to a pressure of carbon monoxide at room temperature reduces the metal dispersion, which in turn reduces the uptake of carbon monoxide, oxygen, and hydrogen. More surface palladium is lost as the carbon monoxide pressure and temperature are increased. The drop in dispersion does not result from the blocking of sites by strongly adsorbed carbon monoxide or by adsorbed carbon. Moreover, the drop in dispersion does not result from the agglomeration of the metal crystallites. The missing sites are regained by oxidation at 550°C, provided the exposure to carbon monoxide is at room temperature and is below 150 Torr CO. These changes in dispersion are slightly more pronounced on the small metal particles.

Effect of Gas Treatments on the Surface Structure

The effect of CO cycling and oxidation on the surface structure of the palladium crystallites was probed by infrared spectroscopy of adsorbed carbon monoxide. We shall first examine the infrared spectra for samples 11b, 11c, and 12b shown in Figs. 3, 4, and 5, respectively. These samples exhibit dispersions ranging from 70 to 37% in the oxidized state and contain relatively small particles of palladium. The infrared spectra of the CO-cycled state of the three catalysts exhibit bands at 2082 and 1970 cm^{-1} . The 1970- cm^{-1} peak contains a broad shoulder on the low-frequency side which probably consists of two peaks of diminishing intensity at 1925 and 1875 cm^{-1} . The shape of this shoulder is the only recogniz-

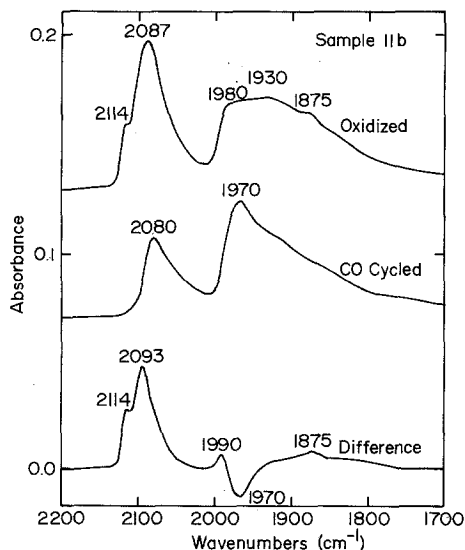


FIG. 3. Infrared spectra of adsorbed carbon monoxide on sample 11b in the oxidized state and in the CO cycled state. The difference spectrum equals the oxidized spectrum minus the CO cycled spectrum.

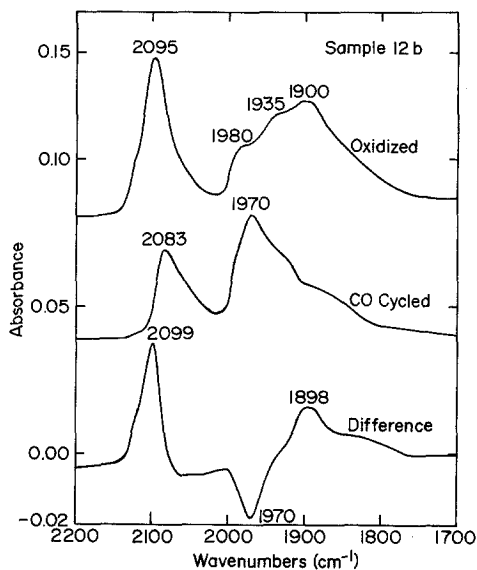


FIG. 5. Infrared spectra of adsorbed carbon monoxide on sample 12b in the oxidized state and in the CO cycled state. The difference spectrum equals the oxidized spectrum minus the CO cycled spectrum.

able difference between the infrared spectra of the CO-cycled state of these catalysts.

The infrared spectra of the CO-cycled

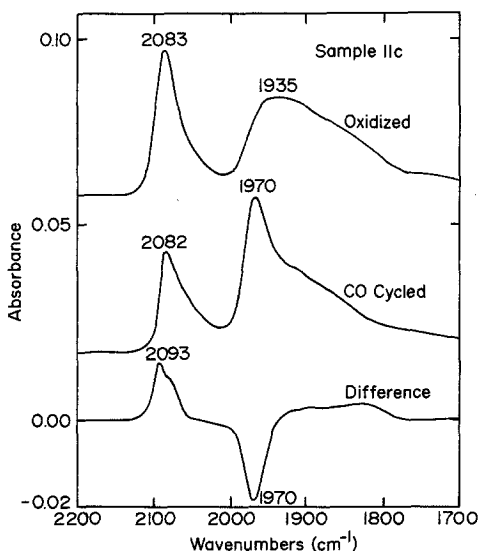


FIG. 4. Infrared spectra of adsorbed carbon monoxide on sample 11c in the oxidized state and in the CO cycled state. The difference spectrum equals the oxidized spectrum minus the CO cycled spectrum.

state of samples 11b, 11c, and 12b are very similar to those observed in previous studies of palladium catalysts (4–6, 20). By analogy to the infrared spectra of carbon monoxide adsorbed on palladium single crystals (10, 21, 22), the peak at 1970 cm^{-1} and the shoulder at 1925 cm^{-1} may be assigned to a carbon monoxide bridge bonded to (100) and (111) facets, respectively, on the palladium crystallites (4, 6, 9). The assignment of the low-frequency peak to carbon monoxide adsorbed on (111) facets was recently confirmed by infrared spectroscopy of coadsorbed carbon monoxide and ethylidyne (7). The other, smaller band at 2082 cm^{-1} is due to linearly bonded carbon monoxide on planes, corners, edges, and defect sites of the particles (4). Based on these assignments, and the distribution of the peaks observed in the spectra, the small palladium particles in the CO-cycled state appear to be terminated by smooth, low index planes.

The infrared spectra of the oxidized state of samples 11b, 11c, and 12b exhibit a large peak near 2090 cm^{-1} and a broadband extending from 2000 to 1800 cm^{-1} . The broad

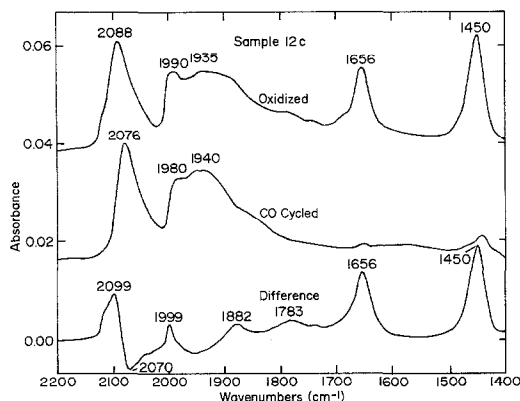


FIG. 6. Infrared spectra of adsorbed carbon monoxide on sample 12c in the oxidized state and in the CO cycled state. The difference spectrum equals the oxidized spectrum minus the CO cycled spectrum.

band is made up of peaks at approximately 1980, 1935, 1900, and 1875 cm^{-1} . The shape of this band varies from sample to sample. Also shown in each figure is a difference spectrum, which is obtained by subtracting the CO-cycled spectrum from the oxidized spectrum. The difference spectra show that on transforming the samples from the CO-cycled state to the oxidized state, the 1970- cm^{-1} peak disappears and is replaced by large peaks near 2095 cm^{-1} . This redistribution of intensities corresponds to replacing carbon monoxide bridge bonded to Pd(100) with carbon monoxide linearly bonded to low coordination sites. Apparently, oxidation at 550°C converts the (100) facets on the crystallites into rough, disordered surfaces.

Shown in Fig. 6 are the infrared spectra for sample 12c. This sample exhibits a dispersion of 15% after oxidation and contains large particles of palladium. The infrared spectrum of the CO cycled state is dominated by the peak for linearly adsorbed carbon monoxide at 2076 cm^{-1} . This indicates that a good portion of the palladium surface is composed of steps, edges, defects, and other low-coordination sites. The band for bridge-bonded carbon monoxide is made up of nearly equal contributions of the peaks at 1980 and 1940 cm^{-1} . A distribution of facets

on the metal particles consistent with these intensities is half (100) and half (111).

The difference spectrum shows that on converting sample 12c from the CO-cycled state to the oxidized state, infrared peaks at 2099, 1999, 1882, 1783, 1656, and 1450 cm^{-1} increase in intensity, while the infrared peak at 2070 cm^{-1} decreases in intensity. The 1656- and 1450- cm^{-1} peaks grow the most. They are due to the symmetric and asymmetric stretching modes of a surface carbonate (23). These bands do not appear on alumina after it is oxidized at 900°C, reduced at 300°C, and exposed to carbon monoxide. O'Neill and Yates (24) observed these bands when nickel oxide supported on alumina was contacted with carbon monoxide and assigned them to carbonate bound to the nickel oxide. An alternative explanation, which we prefer, is that the carbonate forms on the alumina on sites created by an interaction of the metal with the support during catalyst preparation. However, additional experiments must be done to determine whether this is true.

Small bands at 1656 and 1450 cm^{-1} are observed for the other catalyst samples in the oxidized state. The bands are always larger for the "c" series samples than for the "b" series samples, and therefore, are linked to the initial oxidation at 900°C (see Table 1). Nevertheless, only on sample 12c do the intensities of the carbonate peaks grow to larger than 10% of the intensities of the peaks for carbon monoxide on palladium.

The 2099-, 1999-, and 1882- cm^{-1} absorbances observed in the difference spectrum of sample 12c are due to linear, bridge, and threefold-bridge attachment of carbon monoxide to palladium. These bands have been detected previously for adsorption of carbon monoxide on Pd(111) at 90 K (10) and on Pd/SiO₂ at 80 K (25). In the latter study, the authors observed, at high coverages, a stoichiometric conversion of two bridge-bonded carbon monoxide molecules into two linearly bonded carbon monoxide molecules with the adsorption of a third carbon

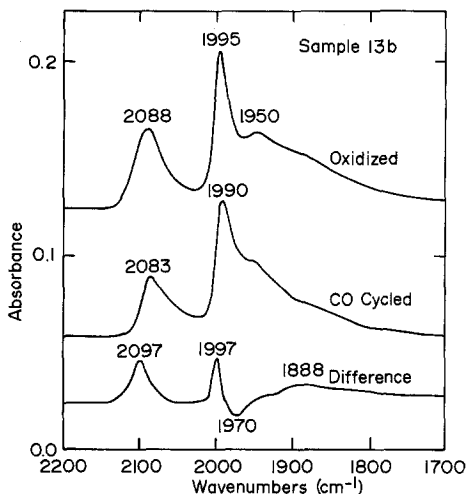


FIG. 7. Infrared spectra of adsorbed carbon monoxide on sample 13b in the oxidized state and in the CO cycled state. The difference spectrum equals the oxidized spectrum minus the CO cycled spectrum.

monoxide molecule. The increased coverage results in bridge and linear bonding of carbon monoxide to the same palladium atom, and it is these species which yield the 1999- and 2099- cm^{-1} peaks. By the same reasoning, the peak at 1882 cm^{-1} may be assigned to threefold-bridge-bonded carbon monoxide sharing a palladium atom with linearly bonded carbon monoxide.

In the previous two studies (10, 25), the sites giving rise to 2099-, 1999-, and 1882- cm^{-1} peaks are occupied by crowding carbon monoxide onto crystal planes at 80 or 90 K. However, on our catalysts, these sites are occupied at room temperature. We propose that our catalysts contain rough surfaces, similar to highly stepped single crystals. Shared bonding to palladium occurs at the step, with linear attachment of carbon monoxide to the step atom and bridge attachment of carbon monoxide to the adjacent terrace site. An infrared study of carbon monoxide adsorption on stepped Pd(100) and Pd(111) is needed to validate these assignments. Nevertheless, this interpretation is consistent with the surface of

the palladium particles becoming rougher after oxidation at 550°C.

Shown in Fig. 7 are the infrared spectra for sample 13b. This catalyst exhibits a dispersion of 9% after oxidation. The CO-cycled and oxidized states exhibit similar infrared spectra, with peaks at 2085, 1995, and 1950 cm^{-1} . The difference spectrum shows that conversion to the oxidized state increases the intensity of the 2097- and 1997- cm^{-1} bands and decreases slightly the intensity of the 1970- cm^{-1} band. These changes are consistent with a portion of the (100) facets transforming into a disordered surface structure.

Shown in Fig. 8 are the infrared spectra for sample 13c. This catalyst exhibits a dispersion of 3% after oxidation. It contains the largest palladium particles of the six samples studied. The infrared spectrum of the CO-cycled state shows two peaks at 2050 and 1955 cm^{-1} . The distribution of intensities is characteristic of linear and bridge bonding of carbon monoxide to surfaces composed mostly of (111) facets. Conversion to the

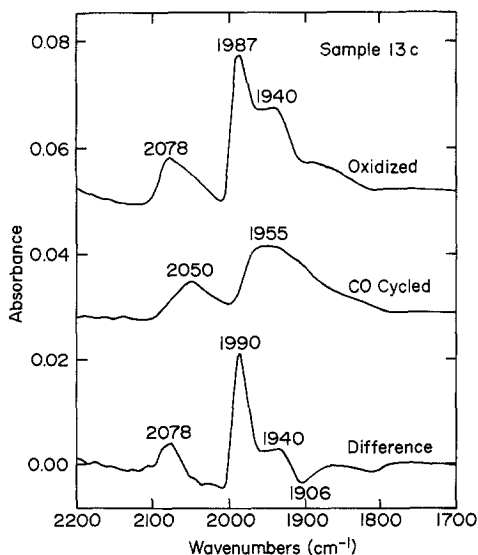


FIG. 8. Infrared spectra of adsorbed carbon monoxide on sample 13c in the oxidized state and in the CO cycled state. The difference spectrum equals the oxidized spectrum minus the CO cycled spectrum.

oxidized state produces a relatively large increase in the intensity of bands at 2078, 1990, and 1940 cm^{-1} . The peak at 1990 cm^{-1} is similar to that observed at high carbon monoxide coverages on Pd(210) and Pd(100) single crystals (10). These results indicate that oxidation of sample 13c generates additional facets on the crystallites which are of a more open geometry than the (111) planes.

To summarize, the infrared spectra of adsorbed carbon monoxide reveal that the surface structure of the palladium crystallites is strongly affected by the gas treatments. Oxidation at 550°C roughens the metal surfaces. The uneven structure persists through hydrogen reduction at 300°C and adsorption of carbon monoxide at 25°C. On exposure of the catalyst to carbon monoxide gas at room temperature, the rough surfaces transform into smooth planes of mainly (100) orientation. There are exceptions to this trend, however. Oxidation of sample 12c at 550°C generates a large number of sites which convert carbon monoxide into adsorbed carbonate. These sites may be on palladium oxide or on alumina. Oxidation of sample 13c at 550°C increases the number of facets exposed on the palladium particles. These facets exhibit an open geometry similar to a (210) or a (100) orientation.

Model for the Restructuring of Palladium Crystallites

Our results can be explained by a rearrangement of the atoms on the surface of the palladium crystallites. A model for this process is shown in Fig. 9. After oxidation, the surface is rough. Contacting the catalyst with carbon monoxide gas at room temperature smooths away the irregularities, converting the surface into low-index crystal facets. The process is reversible provided the exposure is at room temperature and the pressure of carbon monoxide is well below 760 Torr.

For the two-dimensional particles shown in Fig. 9, the unshaded atoms on the perimeter make up the "surface," while the shaded atoms in the center make up the "bulk."

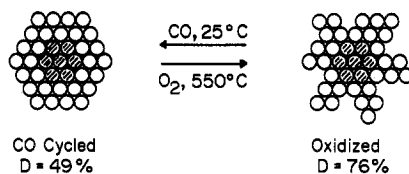


FIG. 9. A model for the restructuring of the palladium crystallite surfaces. Carbon monoxide exposure at 25°C followed by reduction at 300°C smooths the surfaces, whereas oxidation at 550°C followed by reduction at 300°C roughens them. Surface atoms are unshaded; bulk atoms are shaded.

The particle in the oxidized state exhibits a dispersion of 76% (28 Pd_s/37 Pd_t), whereas the particle in the CO-cycled state exhibits a dispersion of 49% (18 Pd_s/37 Pd_t). Both particles show the same number of bulk atoms because both particles dissolve the same amount of hydrogen. If infrared spectra were recorded of carbon monoxide adsorbed on these particles, the oxidized state would show larger peaks for linearly bonded carbon monoxide at 2095 cm^{-1} and for bridge-bonded carbon monoxide at 1995 and 1882 cm^{-1} . All of these trends are consistent with the adsorption characteristics exhibited by the palladium on alumina catalysts.

Prior studies of palladium oxidation support the model of surface roughening. Chen and Ruckenstein (26–28) took electron micrographs of alumina-supported palladium particles after heating them to different temperatures in oxygen. Extensive fragmentation and pitting of the particles occurs during oxidation between 350 and 870°C. Upon reduction at 550°C, the fragments collapse together to form crystallites of about the same size as those present before oxidation (28). This confirms that no change in the size of the palladium crystallites occurs following oxidation at 550°C and reduction at 300°C. Lattice imaging and optical diffraction in the electron microscope reveal that the fragments of oxidized palladium mainly consist of fcc metal (29). The oxide is limited to a thin film covering the exterior of the metal cores (17). Campbell *et al.* (30) found that the surface of palladium foil roughens and

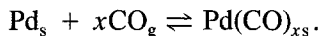
develops pits during oxidation. To achieve tetrahedral coordination of oxygen about each metal atom as occurs in palladium oxide (31), the metal atoms must move far from their original positions. During reduction at 300°C, the metal atoms cannot reorganize into low-index crystal planes, and as a result, the surface remains disordered.

Datye and co-workers (32, 33) have observed similar changes in the morphology of silica-supported rhodium crystallites with repeated cycles of oxidation and reduction. Oxidation at 500°C followed by reduction at temperatures below 300°C produces polycrystalline rhodium particles with many grain boundaries and considerable surface roughness. The roughness can be removed by reduction in hydrogen between 400 and 600°C. Braunschweig *et al.* (33) also showed that the change in surface structure affects the catalytic properties of the rhodium.

In an earlier study (17), we determined how much palladium oxidizes when the catalysts are equilibrated in 110 Torr O₂ at 300°C. The amount of oxygen adsorbed under these conditions far exceeds the number of surface atoms, indicating that a portion of the bulk palladium oxidizes. The extent of oxidation increases with decreasing particle size and increasing crystal imperfections. The effect of carbon monoxide exposure, oxidation, and reduction on the extent of oxidation at 300°C and 110 Torr O₂ was examined in the present study. The amount of oxygen adsorbed remains constant irrespective of whether the sample is exposed to carbon monoxide at 25°C and reduced at 300°C or is oxidized at 550°C and reduced at 300°C prior to the adsorption experiment. Hence, CO cycling and oxidation do not affect the overall structure of the palladium particles, i.e., their size, shape, and degree of crystallinity, since these variables determine how much oxide forms on the particles at 300°C.

A tentative explanation of the restructuring of the palladium on exposure to carbon monoxide at room temperature is as follows.

A mobile palladium carbonyl species forms in the presence of carbon monoxide gas and palladium metal:



This carbonyl species exists only on the surface of the particles and decomposes on desorption into the vapor. It can be considered a less stable chemical analog to nickel tetracarbonyl, which is a liquid at room temperature (34). The rearrangement of metal atoms is driven by the minimization of the surface free energy of the particles. The mobile palladium carbonyls move from positions of low coordination number to those of high coordination number, thereby smoothing out the uneven surface. The free energy of formation of the palladium carbonyl should be negative, because raising the temperature accelerates the restructuring of the crystallites.

The model of surface restructuring needs to be verified by further experimentation. High-resolution electron microscopy would be most helpful, since it would provide visual confirmation of the changes in morphology. The effects of catalyst preparation and support composition should be studied to assess the generality of this phenomenon. In addition, the assignments of the infrared bands for adsorbed carbon monoxide should be checked against studies of stepped single crystals of palladium.

Implications for Catalyst Design

The reversible transformation from smooth crystallites to rough ones provides a way of tailoring the catalytic properties of palladium. For a structure-insensitive reaction, oxidation can be used to roughen the particles and increase the amount of exposed palladium. Conversely, for a structure-sensitive reaction, which proceeds at a high rate on low-index crystal facets, carbon monoxide exposure can be used to smooth out the particles and increase the percentage of the surface oriented in (100) and (111) planes.

A difference in the catalytic activity of the oxidized state and the CO-cycled state is observed for the oxidation of adsorbed carbon. Shown in Fig. 2 are the temperature-programmed oxidation spectra for removal of residual carbon on the catalysts. The temperature of the maximum rate of carbon dioxide formation is about 45°C lower on palladium in the oxidized state than in the CO-cycled state. Evidently, adsorbed carbon oxidizes at a faster rate on the rough palladium surfaces.

Surface restructuring may play a role in catalytic reactions which either consume or produce carbon monoxide. Regardless of the initial condition of the catalyst, exposure to carbon monoxide during reaction should convert the palladium particles into the CO-cycled state. Baddour *et al.* (35) reported a "break-in" phenomenon for carbon monoxide oxidation over silica-supported palladium. The infrared spectrum they recorded before reaction is characteristic of palladium in the oxidized state, since it contains a broad low-frequency band with maxima occurring at 1965, 1940, 1920, and 1885 cm^{-1} . During reaction in several Torr of oxygen and carbon monoxide at 200°C, the infrared spectrum slowly changes to a shape characteristic of palladium in the CO-cycled state. The low-frequency band in this spectrum consists of a main peak at 1985 cm^{-1} and a shoulder at 1965 cm^{-1} . Baddour *et al.* (35) observed a large decrease in the apparent activation energy with break-in, although the rate of reaction remained fairly constant. They attributed the break-in phenomenon to a structural rearrangement of the palladium surface.

Often the variation in rate with particle size is used to gauge the structure-sensitivity of catalytic reactions (36). However, the infrared spectra shown in Figs. 3 through 8 reveal that the surface structure can be quite similar on particles of widely varying size. For example, compare the infrared spectra of the oxidized states of sample 11b (dispersion 70%) and sample 12b (dispersion 37%).

Except for a subtle difference in the shape of the band for bridge-bonded carbon monoxide, the infrared spectra of these samples exhibit a similar distribution of peak intensities. A better test of structure-sensitivity may be to measure the reaction rate over sample 13c in both the CO-cycled and the oxidized states. Although the dispersion changes little between these two states, the infrared spectra in Fig. 8 indicate large differences in the surface structure.

CONCLUSIONS

After the initial oxidation at 700 or 900°C and reduction at 300°C, the palladium on alumina catalysts exhibit dispersions ranging from 3 to 86%. Repeated cycling between carbon monoxide exposure at room temperature and reduction at 300°C lowers the dispersion of all the samples by 20 to 50%. Small crystallites exhibit larger drops in dispersion. The lost adsorption sites can be recovered by oxidation at 550°C and reduction at 300°C, provided the carbon monoxide exposure is at room temperature and below 760 Torr. The hydrogen solubility in the bulk of the palladium crystallites is unaffected by CO cycling. Infrared spectroscopy of adsorbed carbon monoxide shows that CO cycling increases the amount of carbon monoxide bridge bonded to (100) facets, while it decreases the amount of carbon monoxide linearly bonded to low coordination sites.

These results are consistent with the reversible interconversion of rough palladium surfaces into smooth ones with cycling between oxidation at 550°C and carbon monoxide exposure at 25°C. The metal atoms move to new coordination sites when the outer layers of the crystallites are oxidized at 550°C. Reduction at 300°C does not anneal out the surface irregularities generated by oxidation. However, carbon monoxide exposure, possibly through the formation of a mobil palladium carbonyl species, smooths away the imperfections, reforming the low

index crystal facets. Further experiments should be performed to verify this model of the process.

Surface restructuring may be used to enhance the catalytic activity of palladium. Oxidation and reduction can roughen the surface to increase the number of sites for structure-insensitive reactions. Conversely, carbon monoxide exposure and reduction can increase the number of oriented facets on the crystallites for structure-sensitive reactions.

ACKNOWLEDGMENTS

This work was supported by a National Science Foundation Research Initiation Award and by a contract with the Gas Research Institute (No. 5086-260-1247).

REFERENCES

1. Anderson, J. R., "Structure of Metallic Catalysts." Academic Press, New York (1975).
2. Farrauto, R. J., *AIChE Symp. Ser.* **143**, **70**, 9 (1974).
3. Benson, J. E., Hwang, H. S., and Boudart, M., *J. Catal.* **30**, 146 (1973).
4. Hicks, R. F., Yen, Q. J., and Bell, A. T., *J. Catal.* **89**, 498 (1984).
5. Eischens, R. P., and Pliskin, W. A., in "Advances in Catalysis" (D. D. Eley, W. G. Frankenburg, and V. I. Komarewsky, Eds.), Vol. 10, p. 1. Academic Press, San Diego, 1958.
6. Palazov, A., Kadinov, G., Bonev, Ch., and Shopov, D., *J. Catal.* **74**, 44 (1982).
7. Beebe, T. P., and Yates, J. T., *Surf. Sci.* **173**, L606 (1986).
8. Greenler, R. G., Burch, K. D., Kretzschmar, K., Klauser, R., Bradshaw, A. M., and Hayden, B. E., *Surf. Sci.* **152/153**, 338 (1985).
9. Sheppard, N., and Nguyen, T. T., in "Advances in Infrared and Raman Spectroscopy" (R. J. H. Clark and R. E. Hester, Eds.), p. 67. Heyden & Son, London, 1978.
10. Hoffmann, F. M., *Surf. Sci. Rep.* **3**, 107 (1983).
11. Bradshaw, A. M., and Schweizer, E., in "Advances in Spectroscopy: Spectroscopy of Surfaces" (R. J. H. Clark and R. E. Hester, Eds.), p. 413. Wiley, New York, 1988.
12. Chou, P., and Vannice, M. A., *J. Catal.* **104**, 17 (1987).
13. Ichikawa, S., Poppa, H., and Boudart, M., *ACS Symp. Ser.* **248**, 439 (1984).
14. Ichikawa, S., Poppa, H., and Boudart, M., *J. Catal.* **91**, 1 (1985).
15. Rieck, J. S., and Bell, A. T., *J. Catal.* **96**, 88 (1985).
16. Rieck, J. S., and Bell, A. T., *J. Catal.* **103**, 46 (1987).
17. Hicks, R. F., Qi, H., Young, M. L., and Lee, R. G., H., *J. Catal.* **122**, 295 (1990).
18. Boudart, M., and Hwang, H. S., *J. Catal.* **39**, 44 (1975).
19. Wicke, E., and Nernst, G. H., *Ber. Bunsenges Phys. Chem.* **68**, 224 (1964).
20. Palazov, A., Chang, C. C., and Kokes, R. J., *J. Catal.* **36**, 338 (1975).
21. Bradshaw, A. M., and Hoffmann, F. M., *Surf. Sci.* **72**, 513 (1978).
22. Ortega, A., Hoffmann, F. M., and Bradshaw, A. M., *Surf. Sci.* **119**, 79 (1982).
23. Little, L. H., "Infrared Spectra of Adsorbed Species," p. 74. Academic Press, New York, 1966.
24. O'Neill, C. E., and Yates, D. J. C., *Spectrochim. Acta* **17**, 953 (1961).
25. Gelin, P., Siedle, A. R., and Yates, J. T., *J. Phys. Chem.* **88**, 2978 (1984).
26. Ruckenstein, E., and Chen, J. J., *J. Catal.* **70**, 233 (1981).
27. Chen, J. J., and Ruckenstein, E., *J. Phys. Chem.* **85**, 1606 (1981).
28. Ruckenstein, E., and Chen, J. J., *J. Colloid Interface Sci.* **86**, 1 (1982).
29. Jacobs, J. W. M., and Schryvers, D., *J. Catal.* **103**, 436 (1987).
30. Campbell, C. T., Foyt, D. C., and White, J. M., *J. Phys. Chem.* **81**, 491 (1977).
31. Bayer, G., and Wiedemann, H. G., *Thermochim. Acta* **11**, 79 (1975).
32. Chakraborti, S., Datye, A. K., and Long, N. J., *J. Catal.* **108**, 444 (1987).
33. Braunschweig, E. J., Logan, A. D., Chakraborti, S., and Datye, A. K., in "Proceedings, 9th International Congress on Catalysis, Calgary, 1988" (M. J. Phillips and M. Ternan, Eds.), p. 1122. Chem. Institute of Canada, Ottawa, 1988.
34. Cotton, F. A., and Wilkinson, G., "Advanced Inorganic Chemistry," p. 1051. Wiley, New York, 1980.
35. Baddour, R. F., Modell, M., and Goldsmith, R. L., *J. Phys. Chem.* **74**, 1787 (1970).
36. Boudart, M., and Djega-Mariadassou, G., "Kinetics of Heterogeneous Catalytic Reactions." Princeton Univ. Press, Princeton, NJ, 1984.